

[« Back to Article View](#)

Databases selected: Multiple databases...

Controlled local delivery of interleukin-2 by biodegradable polymers protects animals from experimental brain tumors and liver tumors

Justin Hanes, Allen Sills, Zhong Zhao, Kwang Wook Suh, et al. *Pharmaceutical Research*. New York: Jul 2001. Vol. 18, Iss. 7; pg. 899

Author(s): Justin Hanes, Allen Sills, Zhong Zhao, Kwang Wook Suh, et al

Article types: General_Information

Section: Research paper

Publication title: *Pharmaceutical Research*. New York: Jul 2001. Vol. 18, Iss. 7; pg. 899

Source Type: Periodical

ISSN/ISBN: 07248741

ProQuest document ID: 390358691

Text Word Count 6311

Article URL: http://gateway.proquest.com/openurl?ctx_ver=z39.88-2003&res_id=xri:pqd&rft_val_fmt=ori:fmt:kev:mtx:journal&genre=article&rft_id=xri:pqd:did=000000390358691&svc_dat=xri:pqi:fmt=tex&req_dat=xri:pqi:pq_clntid=19649

Full Text (6311 words)

Copyright Kluwer Academic Publishers Jul 2001

[Headnote]

Received March 19, 2001; accepted April 2, 2001

Purpose. The purpose of our study was to develop an injectable polymeric system for the long-term localized delivery of bioactive interleukin-2 for antitumor immunotherapy.

Methods. IL-2 was encapsulated into gelatin and chondroitin-6sulfate using an aqueous-based complex coacervation. CTLL-2 cells were used to measure the bioactivity of released IL-2 and radiolabeled IL-2 was used for release studies in the rat brain and mouse liver. Antitumor efficacy studies were carried out in primary (9L gliosarcoma) and metastatic (B16-F10 melanoma) brain tumor models in rats and mice, respectively, as well as a murine liver tumor model (CT26 carcinoma). Survivors of the metastatic brain tumor challenge were rechallenged with tumor in the opposite lobe of the brain to confirm that antitumor immunologic memory had developed.

Results. Bioactive IL-2 was released for over 2 weeks in vitro and in vivo IL-2 release showed significant IL-2 levels for up to 21 days. Polymeric IL-2 microspheres injected intratumorally were statistically more effective in protecting animals challenged with fatal tumor doses in the brain and the liver than placebo or autologous tumor cells genetically engineered to secrete IL-2. Immunologic memory was induced following IL-2 microsphere therapy in the B16-F10 brain tumor model that was capable of protecting 42% of animals from a subsequent intracranial tumor challenge, suggesting that tumor destruction was mediated by the immune system.

Conclusions. Local IL-2 therapy using novel polymeric carriers, aimed at stimulating long-lasting antitumor immunity, may provide an improved method of treating a variety of cancers.

KEY WORDS: polymer microspheres; interleukin-2; controlled release; immunotherapy; brain cancer; liver cancer.

[Headnote]

ABBREVIATIONS: CNS, central nervous system; IC, intracranial; B16/IL-2, replication-incompetent B16-F10 tumor cells genetically engineered to secrete IL-2; CT26/IL-2, replication-incompetent CT26 tumor cells genetically engineered to secrete IL-2.

INTRODUCTION

Advances in molecular biology have spurred renewed interest in using the body's own defenses to fight cancer, as several potent stimulators of the immune system (cytokines) have been cloned and are now available for use. Interleukin-2 (IL-2) was one of the first cytokines to be cloned and has a number of

activities associated with it, including the enhancement of T cell growth, T cell activation, monocyte activation and natural killer cell activation (1). IL-2 is currently indicated for systemic administration to treat adult patients with melanoma and metastatic renal cell carcinoma. A major limitation of this treatment, however, is the severe toxicity caused by high doses of systemic IL-2 (2).

The major conceptual problem with systemic cytokine administration is that lymphokines are known to exert their immunologic effects locally, in a paracrine fashion (2). That is, under normal physiologic conditions, appropriate lymphokines are produced in high concentrations local to the site of antigen where they serve as the necessary costimulatory signal for induction of an appropriate immune response. This paracrine function cannot be achieved when cytokines are administered systemically. Toxicity from systemic administration of IL-2 can also be severe and would be particularly limiting in the treatment of brain tumors, as the availability of macromolecules to the brain is limited by the blood-brain barrier (3).

Most recent efforts to deliver molecules, such as IL-2, locally to tumors in both the brain (4,5) and the periphery (for review see (6)) have focused on the use of autologous tumor cells genetically engineered to secrete cytokines, often with promising results. Local cytokine delivery by genetically engineered cells is not only physiologically more relevant, but also allows high concentrations of the stimulatory molecule at the tumor site while greatly reducing systemic exposure. However, while conceptually elegant, this approach is difficult to implement in the clinic due to the labor intensity and high cost involved with the genetic transduction of each patient's tumor cells and due to the extensive characterization of the transductants required before they may be used. (7). In addition, there may be inherent variability with cytokine-producing cells that are rapidly destroyed by the immune system following administration.

In this article, we discuss the development of an injectable polymeric system capable of delivering active recombinant IL-2 in a controlled fashion following intratumoral injection for up to 21 days in vivo. Moreover, we show that local IL-2 delivery from microspheres, made by the complex coacervation of gelatin and chondroitin sulfate, can effectively protect rats and mice from lethal tumor challenges in three different tumors models (two model brain tumors and one model liver tumor). Gelatin (denatured collagen) and chondroitin sulfate (CS) were used to encapsulate IL-2 for three reasons. First, collagen and chondroitin sulfate are primary components of extracellular matrix (ECM) and, thus, systems made using gelatin and CS should be biocompatible. Second, gelatin and CS can be made to coacervate and entrap proteins under mild, all-aqueous conditions that should improve activity retention of sensitive proteins, such as IL-2. Finally, tumors typically secrete degradative enzymes, including collagenase, to degrade ECM in order to grow and metastasize (8). In doing so, actively growing tumors may cause an increased rate of polymer degradation, thereby exposing themselves to higher IL-2 concentrations.

Polymeric microspheres may provide a more controlled product with respect to cytokine release profiles and total cytokine dose than can be achieved with genetically engineered cells or by in vivo gene therapy, thereby providing an improved method of administering therapeutic gene products (i.e. proteins). Furthermore, the use of polymeric microspheres to deliver IL-2 may simplify therapy by eliminating the need for transfection of each patient's cells with cytokine genes. The development of such a system would allow clinicians to administer cytokine immunotherapy at the time of surgical debulking of an existing tumor, obviating the need to reoperate many days to weeks later to administer genetically engineered autologous cells. Because gelatin (denatured collagen) and chondroitin sulfate both occur naturally in the body, the polymeric delivery system described in this study may be suitable for the immunotherapy of many solid tumors.

MATERIALS AND METHODS

Synthesis of Polymeric IL-2 Delivery Vehicle

IL-2 was encapsulated into polymeric matrices (IL-2 microspheres) by the complex coacervation of gelatin and chondroitin-6-sulfate in the presence of IL-2. Edible porcine gelatin (100 Bloom) was supplied by General Foods (Atlantic Gelatin, Woburn, MA). Chondroitin-6-sulfate and glutaraldehyde were purchased from Sigma Chemical Co. (St. Louis, MO). Briefly, 3 ml of a 4% gelatin solution in distilled water at 37[degrees]C was mixed with 1 mg of lyophilized IL-2 dissolved in 3 ml of 0.2% chondroitin sulfate in phosphate buffer solution at room temperature. Coacervation was achieved by the addition of the gelatin solution to a rapidly mixed IL-2/ chondroitin sulfate solution. Nascent microspheres were cross-linked with 0.125% aqueous glutaraldehyde solution for 20 min and then poured into 10 ml of a 0.1M aqueous glycine solution to stop the cross-linking reaction and quench the excess aldehyde groups. Crosslinked microspheres were collected by centrifugation and washed with phosphate-buffered saline. Placebo microspheres were prepared identically, but in the absence of IL-2.

The mass-average diameter of the microspheres was determined using a Coulter Multisizer II (Coulter Electronics, Luton, Beds, England). Greater than 200,000 microspheres were sized per measurement (n 4 3 batches).

Preparation and Encapsulation of 125I-Labeled IL-2

Na¹²⁵I in 0.1N NaOH was obtained from NEN Life Science Products (Boston, MA). Recombinant IL-2 (Aldesleukin, 22 million IU per 1.3 mg protein) was kindly supplied by Chiron Corporation (Emeryville, CA). ¹²⁵I was covalently attached to IL-2 by reaction in a pre-coated iodination tube (Iodogent, Pierce, Rockford, IL) for 10 min. Unreacted ¹²⁵I was separated from ¹²⁵I-labeled IL-2 ([¹²⁵I]IL-2) by column chromatography (Econo-Pak 10DG column, BioRad, Hercules, CA). Radiolabeled [¹²⁵I]IL-2 was subsequently encapsulated into gelatin/chondroitin sulfate microspheres following the standard encapsulation procedure described above and used to determine the IL-2 encapsulation efficiency and the in vivo release kinetics of IL-2 following intracranial or intrahepatic injection in rats and BALB/c mice, respectively.

Tumor Cells

9L gliosarcoma cells and CT26 colon carcinoma cells were obtained from ATCC and B16-F10 melanoma cells were obtained from the National Cancer Institute Division of Cancer Treatment and Diagnosis Tumor Repository (Frederick, MD). Tumor cells were maintained in Dulbecco's modified Eagle's medium (DMEM) containing 10% FCS and penicillin/ streptomycin in humidified incubators at 37[degrees]C and gassed with 5% carbon dioxide. The B16-F10 and CT26 cell lines were transduced with the murine IL-2 gene by using the replicationdefective MFG retroviral vector, as previously described (9). The amount of IL-2 produced by transformed tumor cells was quantified routinely using a standard ELISA kit (Endogen, Cambridge, MA). Cultured tumor monolayers were harvested with 0.025% trypsin, counted, and resuspended in DMEM prior to inoculation. Transduced tumor cells were exposed to 5000 rads (1 rad 4 0.01 Gy) from a ¹³⁷Cs source (Gammacell model 62 irradiator, Nordin International, Inc., Kanata, Ontario, Canada) discharging approximately 1300 rads/min to render them replication-incompetent immediately prior to injection.

Animals

The use of animals in this study was carried out in accordance with the "Principles of Laboratory Animal Care" (NIH publication #85-23, revised 1985). Fisher 344 rats weighing 200-250 g, 6-8 week old BALB/c mice, and 6-8 week old C57/B6 mice were obtained from Harlan (Indianapolis, IN) and housed in an approved animal facility. Animals were allowed free access to Purina Rodent Chow and water.

Intracranial and Intrahepatic Injections

Rats and mice were anesthetized prior to all surgical procedures. Rats were anesthetized by an intraperitoneal injection of 1 ml of a stock solution containing ketamine hydrochloride (25 mg/ml), xylazine (2.5 mg/ml), and 14.25% ethyl alcohol. Mice were anesthetized by an intraperitoneal injection of 0.1 ml of this stock solution diluted 1:3 in 0.9% aqueous NaCl solution.

For intracranial injection of tumor cells or polymer microspheres, the head of mice or rats was shaved and prepared with 70% ethanol and iodine-containing solution. A midline incision was made using a scalpel and a 1 mm burr hole was made at the site for injection. All intracranial injections were made in the left parietal lobe of the brain using a stereotactic frame (the coordinates in mice were 2 mm posterior to the coronal suture and 2 mm lateral to the sagittal suture; coordinates in rats were 5 mm posterior and 3 mm lateral to the bregma). Tumor cells or polymer microspheres were delivered over a period of 3 min by a 26-gauge needle inserted to a depth of 3 mm in both mice and rats. The needle was removed following injection and the site was irrigated with 0.9% NaCl solution and closed with 4.0 Vicryl sutures.

For intrahepatic injection of tumor cells or microspheres in BALB/c mice, the abdominal region was shaved and prepared with 70% ethanol and iodine-containing solution. A transverse incision was used to open the peritoneal cavity and the left lobe of the liver was exposed. Using an operative microscope, 10 ml of HBSS containing 5×10^4 wild type CT26 cells (CT26 WT) were injected beneath the liver capsule using a 30-gauge needle. Compression of the liver capsule at the injection site was maintained for one minute to prevent extravasation. 4.0 Vicryl suture was used to close the abdominal incision. Using this method and cell dose, a solitary intraparenchymal tumor can be readily identified by the naked eye by day 2 following tumor injection, and 90% of untreated tumor-bearing animals die by day 28 due to massive hepatic tumor growth (all animals die by day 55). Animals treated by concomitant injection of CT26/IL-2 or IL-2 microspheres received a total injection volume of 13 ml.

In Vivo IL-2 Release from Polymer Microspheres

Polymer microspheres containing [^{125}I]IL-2 were injected intracranially into Fisher 344 rats and into the left lobe of the liver of BALB/c mice to determine the in vivo release kinetics of [^{125}I]IL-2 from the polymeric carrier. Control animals received a bolus injection of free [^{125}I]IL-2.

Groups of rats were given either an intracranial injection of free [^{125}I]IL-2 (i.e. not encapsulated into polymeric carrier) or an identical dose of [^{125}I]IL-2 encapsulated within polymer microspheres in a total volume of 10 ml of PBS. Animals were sacrificed at predetermined time points and their brains removed and frozen prior to sectioning with a cryostat microtome. 20 μm sections were mounted on glass slides, air-dried in a sterile hood and wrapped in a single layer of plastic wrap along with an ^{125}I standard plastic strip (Amersham Pharmacia Biotech, Piscataway, NJ). The slides were subsequently exposed to a phosphorus imager screen (FUJIFILM Medical Systems USA, Stamford, CT) in a sealed cassette and the phosphorus screen processed in a phosphorus imager (MacBas 1000, FUJIFILM Medical Systems USA, Stamford, CT) to yield the IL-2 concentration profiles in each tissue section.

To confirm long-term IL-2 delivery by polymer microspheres in tissues other than the brain, groups of BALB/c mice were injected intrahepatically with either free [^{125}I]IL-2 or [^{125}I]IL-2 microspheres and the total reactivity in the injection lobe followed over time. While still under general anesthesia, three mice from each group were exsanguinated immediately following intrahepatic injection and their blood and organs harvested in the following order: blood (via cardiac puncture), injection lobe of liver,

remainder of liver, heart, lungs, spleen, kidneys, and brain. The organs and blood were weighed and the amount of radioactive IL-2 in each was determined using a gamma counter. The remaining animals were allowed to recover from anesthesia and were returned to their cages. Subsequently, animals from each group were sacrificed at various time points (3 animals per time point per group) and the [125I]IL-2 activity was measured in the injection lobe of the liver, various other organs, and the blood following the above procedure.

Efficacy of Local IL-2 Delivery in Intracranial and Hepatic Tumor Models

For in vivo testing against brain tumors, animals were challenged intracranially with wild-type 9L gliosarcoma cells (Fischer 344 rats) or B16-F10 melanoma cells (C57/B16 mice). Animals were treated with a simultaneous local injection of placebo microspheres (negative control) or IL-2 microspheres. The total dose of bioactive IL-2 delivered within polymer microspheres was approximately 0.4 mg for mice and 4 mg for rats. There were two additional groups in the mouse brain tumor model study: one group of mice received replication-incompetent B16-F10 cells engineered to secrete IL-2 (B16/IL-2) as a positive control and another group received an equal number of replication-incompetent B16-F10 cells (negative control group). Outcome was measured by survival, and all animals were autopsied at the time of death.

For in vivo testing against liver tumors, the anti-tumor effect of locally delivered IL-2 (by either IL-2 microspheres or CT26/IL-2 cells) was measured by its ability to protect animals challenged intrahepatically with CT26 WT from tumor growth. BALB/C mice were challenged by intrahepatic injection with 5×10^4 CT26 carcinoma cells and simultaneously treated by a local injection of placebo microspheres (negative controls, n 4 9), 106 replication-incompetent CT26 cells engineered to secrete IL-2 (CT26/IL-2, positive controls, n 4 10), or IL-2 microspheres (treatment group, n 4 10). 106 replication-incompetent CT26/IL-2 cells had been determined to yield the optimal anti-tumor effect in a preliminary dose escalation study (data not shown). The total dose of bioactive IL-2 delivered within polymer microspheres was approximately 0.4 mg. Three weeks after intrahepatic tumor challenge, animals were euthanized and examined for tumor presence and tumor volumes were measured.

Intracranial Memory Immunity Studies in IL-2 Microsphere-Treated Survivors

C57/B6 mice that survived a B16-melanoma intracranial challenge as a result of local IL-2 microsphere therapy were rechallenged (n 4 12), along with naive control animals (n 4 10), by stereotactic injection with a lethal dose of B16 in the contralateral hemisphere of the brain 75 days after the original treatment with IL-2 microspheres to determine if antitumor immunologic memory had developed. Animals were returned to their cages following surgery and survival assessed. Autopsy was performed to determine cause of death.

Histology

C57/B6 mice challenged intracranially with B16-F10 WT and treated with placebo microspheres, IL-2 microspheres, or B16/IL-2 cells were sacrificed at various time points following challenge for histologic analysis of the challenge site. Brains were harvested, fixed in 10% formalin, serial sectioned in the coronal plane and embedded in paraffin. Microscopic sections were cut at 6 microns and stained with hematoxylin and eosin. Independent pathologic review of all specimens was performed.

RESULTS

IL-2 Encapsulation into Polymer Microspheres

Injectable polymeric matrices containing entrapped IL-2 were made by the complex coacervation of positively-charged gelatin with negatively-charged chondroitin-6-sulfate. Polymer matrices containing IL-2 (IL-2 microspheres) were spherical in shape and had a mass-mean diameter of 8.25 ± 0.25 μ m (Fig. 1). IL-2 encapsulation efficiency, defined as the fraction of total IL-2 that is entrapped within the microspheres during preparation, was $81.4 \pm 0.4\%$. The microspheres contained 2.6% IL-2 by weight.

In Vivo Controlled Release of IL-2 by Polymer Microspheres

¹²⁵I-labeled IL-2 ([¹²⁵I]IL-2) was encapsulated into gelatin/ chondroitin sulfate microspheres to determine the ability of the polymeric carrier to provide sustained IL-2 levels locally following intracranial (Fig. 2) and intrahepatic (Fig. 3) injection in Fisher rats and BALB/c mice, respectively. Control animals received a bolus injection of free [¹²⁵I]IL-2.

IL-2 administered by bolus injection into the brain of rats was rapidly cleared from the injection site (Fig. 2A). One h following intracranial (IC) injection, IL-2 administered as a bolus was found in high concentration at the injection site, and was spread throughout the ipsilateral hemisphere of the brain (Fig. 2A). However, very low IL-2 levels were detected at the injection site just 24 h following IC injection (greater than 90% of IL-2 cleared from the brain at this time), and IL-2 was undetectable at the injection site after 48 h. On the other hand, IL-2 levels remained high at the site of injection for greater than 2 weeks following stereotactic injection of IL-2 microspheres into the brain of rats (Fig. 2B). Very high levels of IL-2 were present after 48 h when IL-2 microspheres were administered, in contrast to bolus administration of IL-2, and therapeutic levels of IL-2 (approximately 1.7 nM) were still present on day 14, as measured by autoradiography.

To determine the suitability of IL-2 microspheres to control the release of IL-2 in a visceral organ, IL-2 release kinetics were also measured in the liver of BALB/c mice. IL-2 levels in the injection lobe of animals receiving IL-2 microspheres remained high for greater than 14 days (17.5% of original dose still in injection lobe on day 14; Fig. 3), with detectable levels still present on day 21. On the other hand, IL-2 administered as a bolus intrahepatic injection was rapidly removed from the injection site (less than 8% of original dose remained in injection lobe after 24 h). In addition, appreciable levels of IL-2 were found in the other lobes of the liver, blood, kidneys, spleen, and other organs within minutes of bolus intrahepatic IL-2 injection. In contrast, IL-2 levels in sites other than the injection lobe of the liver following IL-2 microsphere injection ranged from very low to undetectable (data not shown).

IL-2 Microsphere Efficacy and Immunity Development in Brain Tumor Models

The efficacy of local IL-2 delivery from gelatin/ chondroitin-sulfate microspheres was tested in the treatment of a metastatic B16-melanoma brain tumor model in mice (4) and a primary brain tumor model, 9L gliosarcoma, in rats. B16 and 9L tumors are highly aggressive and poorly immunogenic and, therefore, represent stringent models for the evaluation of new immunotherapeutic approaches to cancer. In the B16 study, 80 mice received a lethal B16 challenge intracranially and were simultaneously treated with a local injection of one of the following: (1) replication-incompetent B16 cells (antigen control); (2) placebo polymer microspheres (polymer control); (3) replication-incompetent B16 cells engineered to secrete IL-2 (B16/IL-2; positive control); or (4) polymer microspheres engineered to deliver IL-2 (experimental group). All animals in the antigen control group succumbed to massive intracranial (IC) tumors by day 21 (median survival 41.7 days, Fig. 4A). Similarly, animals treated with placebo microspheres all died due to large IC tumor with a median survival time of 18 days. Animals receiving IL-2 secreting B16 cells showed a significant prolongation in survival (median survival time of 29 days)

and 9 of 25 mice (36%) were tumor free after 75 days. However, 16 of 18 mice (89%) that received IL-2 microspheres rejected their tumors and survived greater than 75 days (median survival not reached).

Histological analysis of the intracranial injection site in mice challenged with B16 showed massive tumor necrosis with associated lymphocyte infiltrate surrounding distinct IL-2 polymer microspheres (Fig. 5A). Immunohistochemistry showed that the lymphocyte infiltrate included CD4+ and CD8+ T-cells and natural killer cells (not shown). Acute inflammatory cells and macrophages were also present. The cellular infiltrate in response to IL-2 secreting B16/IL-2 cell injection was similar to that seen with IL-2 microspheres (Fig. 5B). On the other hand, placebo polymer microspheres appeared inert within tumor and in the surrounding brain by histology (Fig. 5C).

Mice that survived a B16-melanoma intracranial challenge as a result of local IL-2 microsphere therapy were rechallenged (n 4 12), along with naive control animals (n 4 10), with a lethal dose of B16-melanoma in the contralateral hemisphere of the brain 75 days after the original treatment with IL-2 microspheres to determine if anti-tumor immunologic memory had developed. All animals in the control group (n 4 10) died of massive intracranial B16 tumors by day 20. On the other hand, 5 of 12 (42%) animals previously cured of intracranial B16 survived the contralateral rechallenge despite no further retreatment, establishing that immunologic memory developed in these animals capable of protecting them from subsequent tumor doses.

We also tested the efficacy of IL-2 microspheres against the 9L gliosarcoma brain tumor model in rats. 9L is an aggressive primary brain tumor model of Fisher 344 rat origin. Twenty-four rats received a lethal 9L challenge intracranially and were simultaneously treated with a local injection of one of the following: (1) placebo polymer microspheres (n 4 8); (2) IL-2 polymer microspheres (n 4 8); or (3) IL-2 polymer microspheres plus replication-incompetent 9L cells (n 4 8) (Fig. 4B). Group 3 was added to assess the potential importance of additional tumor antigen on the generation of an anti-tumor immune response. All animals in the placebo control group succumbed to massive intracranial tumors by day 31 (median survival 4 25 days). In contrast, 3 of 8 animals in each group that received IL-2 secreting polymers rejected their tumors and survived greater than 100 days ($p < 0.0001$, unpaired t test). There was no statistical difference in the survival of animals receiving IL-2 polymers alone compared to IL-2 polymers plus irradiated tumor cells (median survival times of 48 days and 54 days, respectively).

IL-2 Microsphere Efficacy in Murine Liver Tumor Model

To confirm the potential usefulness of IL-2 microspheres in tumors outside the CNS, we performed preliminary efficacy studies in mice challenged with a model metastatic liver tumor. Mice challenged with CT26 carcinoma cells intrahepatically were treated with a local injection of placebo microspheres (n 4 9), CT26 cells engineered to secrete IL-2 (n 4 10), or IL-2 microspheres (n 4 10). On day 21, the animals were sacrificed and tumor volume measured (Fig. 6). All animals that received empty microspheres, or IL-2 secreting CT26 cells, had large tumors with mean volumes (+ or - SEM) of 7025 + or - 2354 mm³ and 731 + or - 245 mm³, respectively. On the other hand, 4 of 10 mice that received IL-2 microspheres had no visible tumor, and the other six animals had relatively small tumors (14 + or - 3 mm³, $p < 0.0058$ vs. empty microspheres, $p < 0.0085$ vs. CT26/IL-2 cells, unpaired t test). Tumor-free animals appeared to have normal, healthy livers upon autopsy.

DISCUSSION

In this article, we discuss the development of a polymeric system capable of the prolonged and controlled delivery of IL-2 following peritumoral injection. Polymeric systems have the advantage of

protecting unreleased molecules from rapid degradation *in vivo*, thus prolonging their effective half-lives many fold (10). Controlled release polymer systems are already in clinical use to deliver low-molecular weight chemotherapeutic molecules to treat malignant glioma in human patients (11). Polymers are also currently used to deliver anticancer peptides, such as leuprolide acetate, which is delivered over a period of approximately 1 month to treat patients with prostate cancer (12).

The development of delivery systems for proteins, however, has been relatively slow and more difficult. In fact, only recently has it been shown in clinical trials that a therapeutically relevant protein (human growth hormone) can be effectively delivered from degradable polymer microspheres over a period of a few weeks (13). The difficulty with delivering proteins, such as IL-2, from biodegradable polymers is due in large part to the fact that the conditions typically used to encapsulate molecules into polymers, including elevated temperatures, high surfactant concentrations, or organic solvent and aqueous solvent mixtures, often result in accelerated protein degradation or aggregation (14,15). Moreover, the polymers used most often to encapsulate drugs, the lactide/ glycolide copolymers (PLGA), are hydrophobic and break down into acidic byproducts by hydrolysis in the body, which are potentially deleterious to protein stability (15).

In contrast, we have used an all-aqueous, low-temperature complex coacervation procedure to encapsulate IL-2 that utilizes naturally occurring, hydrophilic polymers (gelatin and chondroitin-6-sulfate) [for a review of coacervation processes, refer to (16)]. It is necessary to use a gentle preparation method to encapsulate IL-2 due to its poor stability during encapsulation using standard procedures (17). Moreover, hydrophilic polymers were chosen to encapsulate IL-2 because it is a hydrophobic protein that may denature when it adsorbs to hydrophobic surfaces, such as PLGA.

In our process, an aqueous solution of negatively charged chondroitin-6-sulfate (CS) containing IL-2 is rapidly added to an aqueous solution of positively charged gelatin under precise conditions of temperature, pH, gelatin, CS, and salt concentration. Only under precise conditions will the positive charge of the gelatin be sufficiently masked by the negative charge of the CS to lead to the precipitation of a colloid solution rich in the two polymers (i.e., microsphere formation). The high encapsulation efficiency of IL-2 into polymer microspheres in this study (>80%) suggests that IL-2 participates in the electrostatic interactions during coacervation. If it did not, one would expect an IL-2 encapsulation efficiency of less than 20%, which is the approximate percentage of the suspension volume attributed to microspheres following coacervation. The recombinant IL-2 used in this study has a reported isoelectric point of 7.75 (18), making it positively charged at the pH used for encapsulation, and thereby suggesting that the IL-2 may interact primarily with negatively charged CS polymer chains during coacervation. The microspheres formed (mean diameter 78 nm) were approximately the same size as a typical cell (70 nm), thus facilitating an intimate mixing with tumor antigen following intratumoral injection.

In vitro bioassay studies involving IL-2 dependent CTLL-2 cells showed that IL-2 retained approximately 50-75% of its original bioactivity over a period of two weeks. IL-2 was delivered from the gelatin/CS microspheres at a similar rate for over 2 weeks in the brain (Fig. 2) and the liver (Fig. 3) of experimental animals, two obviously different organs. The microspheres sustained measurable levels of IL-2 at the injection site for at least 21 days in the liver study. Release points over two weeks were not investigated in the brain, but similarly high levels of IL-2 remained at the injection site in the brain and liver after 14 days. Moreover, the vast majority of IL-2 delivered by microspheres remains in the organ in which they are injected, thereby minimizing the severe systemic toxicity often associated with this cytokine. In contrast, IL-2 was rapidly removed from the injection site when administered as a bolus in both the brain and the liver (>90% cleared within 24 h). Considering the short duration of IL-2 at the site of the tumor following bolus administration, combined with the difficulty inherent with repeat administration in sites such as the brain or liver, it is not surprising that IL-2 is not currently administered

as a local bolus injection to treat cancer.

The fact that encapsulated IL-2 retained its bioactivity upon release *in vivo* is demonstrated by its efficacy in treating animals challenged with one of three different syngeneic tumor models (Figs. 4 and 6). IL-2 microspheres were statistically more effective than an optimized dose of autologous cells engineered to secrete IL-2 in both the CT26 liver tumor model and the B16 melanoma brain tumor model in mice. Genetically-engineered autologous cells are generally considered the gold standard immunotherapy for cancer (2). Placebo microspheres, on the other hand, did not have a significant effect on survival and appeared completely inert in the brain by histological analysis.

Perhaps the most significant advantage of immunotherapeutic approaches to cancer therapy is the potential to develop long-term immunity to the tumor originally treated (6). Others have shown that treatment of tumors in the flank (i.e., non-CNS) with cells genetically-engineered to secrete IL-2 can lead to immunologic memory capable of protecting the animal from a subsequent tumor challenge (19-22). In this article, we show that immunologic memory can be induced against brain tumors in mice by therapy with IL-2 polymer microspheres. This result confirms that tumor destruction in response to IL-2 microsphere therapy is mediated by the immune system.

There have been a few papers that described attempts at the encapsulation of IL-2 into polymeric vehicles intended for tumor immunotherapy (23-25). However, the IL-2 release duration in two of these studies was very brief (less than a few days) (23,24). Furthermore, none of these previous studies showed that IL-2 microspheres were effective against syngeneic tumors or brain tumors in animal models, nor did any investigate the development of immunologic memory as a result of local polymer-delivered IL-2 therapy.

We have recently shown (Suh, K. W., Hanes, J., Brem, H., Leong, K., Pardoll, D. M., and Choti, M., submitted) that IL-2 microspheres are capable of curing animals with established CT26 liver tumors in Balb/C mice. 9 of 12 animals with established liver tumors (1-2 mm in diameter) were cured of their tumors when treated with IL-2 microspheres; all control animals died by day 55 (median survival 43 days) due to liver failure. We have also recently shown that local delivery of chemotherapeutic molecules by polymer matrices implanted intracranially is synergistic in the treatment of model brain tumors in mice when combined with local IL-2 delivery by genetically engineered cells (26). Future studies are aimed at combining this local IL-2 immunotherapy strategy with other promising strategies, such as adoptive transfer of activated lymphocytes (e.g., tumor-infiltrating lymphocytes, lymphokine-activated killer cells, dendritic cells, etc.) (27-30), and locally-delivered chemotherapy (26).

IL-2 microspheres provide a controlled, easy to handle, reliable system for IL-2 delivery that may be administered at the time of surgical tumor debulking. The ability of the polymeric system to maintain elevated levels of IL-2 at the site of injection over long periods of time should provide for the enhancement of its antitumor activity while minimizing systemic toxicity, which has limited the effectiveness of IL-2 immunotherapy to date. Gelatin/chondroitin-sulfate IL-2 microspheres are relatively easy to manufacture in a reproducible manner compared to genetically-engineered cells and, therefore, may represent the next generation of IL-2 delivery systems for cancer immunotherapy.

ACKNOWLEDGMENTS

This project was supported by the National Cooperative Drug Discovery Group (Grant U01-CA52857) of the National Cancer Institutes of Health (Bethesda, MD) and by the 1997-1998 Bonnie Blair/American Brain Tumor Association Postdoctoral Fellowship for Justin Hanes. The authors are grateful to Professor Robert Langer for his critical review of the manuscript.

[Sidebar]

Pharmaceutical Research, Vol. 18, No. 7, 2001

[Sidebar]

0724-8741/01/0700-0899\$19.50/0 (C) 2001 Plenum Publishing Corporation

[Reference]

REFERENCES

1. R. J. Tushinski and J. J. Mule. Biology of cytokines: The interleukins. In V. T. DeVita Jr., S. Hellman, and S. A. Rosenberg (eds.), *Biologic Therapy of Cancer*, 2nd edition, J.B. Lippincott Company, Philadelphia, 1995 pp. 87-94.
2. D. M. Pardoll. Paracrine cytokine adjuvants in cancer immunotherapy. *Annu. Rev. Immunol.* 13:399-415 (1995).
3. W. M. Pardridge. Preface: Overview of brain drug delivery. *Adv. Drug Deliv. Rev.* 15:1-3 (1995).
4. R. C. Thompson, D. M. Pardoll, E. M. Jaffee, M. G. Ewend, M. C. Thomas, B. M. Tyler, and H. Brem. Systemic and local paracrine cytokine therapies using transduced tumor cells are synergistic in treating intracranial tumors. *J. Immunother.* 19:405-413 (1996).
5. T. Lichtor, R. P. Glick, T. S. Kim, R. Hand, and E. P. Cohen. Prolonged survival of mice with glioma injected intracerebrally with double cytokine-secreting cells. *J. Neurosurg.* 83:1038-1044 (1995).
6. D. M. Pardoll. Cancer vaccines. *Nat. Med.* 4:525-531 (1998).
7. C. E. Weber. Cytokine-modified tumor vaccines: An antitumor strategy revisited in the age of molecular medicine. *Cancer Nurs.* 21:167-177 (1998).
8. R. Ruddon. *Cancer Biology*, Oxford Press, New York, 1995 pp. 117-206, 414-416.
9. G. Dranoff, E. Jaffee, A. Lazenby, P. Golumbek, H. Levitsky, K. Brose, V. Jackson, H. Hamada, D. M. Pardoll, and R. C. Mulligan. Vaccination with irradiated tumor cells engineered to secrete murine granulocyte-macrophage colony-stimulating factor stimulates potent, specific, and long-lasting anti-tumor immunity. *Proc. Natl. Acad. Sci. U.S.A.* 90:3539-3543. (1993).
10. R. Langer. Drug delivery and targeting. *Nature Med.* 392:5-10 (1998).
11. H. Brem, S. Piantadosi, P. C. Burger, M. Walker, R. Selker, N. A. Vick, K. Black, M. Sisti, S. Brem, G. Mohr, P. Muller, R. Morawetz, and S. C. Schold. Placebo-controlled trial of safety and efficacy of intraoperative controlled delivery by biodegradable polymers of chemotherapy for recurrent gliomas. *Lancet* 345: 1008-1012 (1995).
12. H. Okada and H. Toguchi. Biodegradable microspheres in drug delivery. *Crit. Rev. Ther. Drug Carrier Syst.* 12:1-99 (1995).
13. O. L. Johnson, J. L. Cleland, H. J. Lee, M. Charnis, E. Duenas, W. Jaworowicz, D. Shepard, A. Shahzamani, A.J.S. Jones, and S.D. Putney. A month-long effect from a single injection of microencapsulated human growth hormone. *Nature Med.* 2:795-799 (1996).
14. R. T. Bartus, M. A. Tracy, D. F. Emerich, and S. E. Zale. Sustained delivery of proteins for novel therapeutic products. *Science* 281:1161-1162 (1998).
15. S. P. Schwendeman, M. Cardamone, M. R. Brandon, A. Klivanov, and R. Langer. Stability of proteins and their delivery from biodegradable polymer microspheres. In S. Cohen and H. Bernstein (eds.), *Microparticulate Systems for the Delivery of Proteins and Vaccines*, Marcel Dekker, Inc., New York, 1996 pp. 1-50.
16. P. B. Deasy. Coacervation-Phase Separation Procedures Using Aqueous Vehicles. *Microencapsulation and Related Drug Processes*, Marcel Dekker, Inc., New York, 1984 pp. 61-96.
17. M. S. Hora, R. K. Rana, J. H. Nunberg, T. R. Tice, R. M. Gilley, and M. E. Hudson. Controlled release of interleukin-2 from biodegradable microspheres. *Biotechnology (N Y)* 8:755-758 (1990).
18. M. A. Giedlin. Proleukint (aldesleukin) recombinant human IL2: Non-clinical investigators' brochure. Emerville, CA: Chiron Corporation, 1996.
19. J. Connor, R. Bannerji, S. Saito, W. Heston, W. Fair, and E. Gilboa. Regression of bladder tumors in mice treated with interleukin 2 gene- modified tumor cells [published erratum appears in *J. Exp. Med.* 1993 Jun 1;177(6):following 1831]. *J. Exp. Med.* 177:1127-1134 (1993).
20. E. R. Fearon, D. M. Pardoll, T. Itaya, P. Golumbek, H. I. Levitsky, J. W. Simons, H. Karasuyama, B. Vogelstein, and P. Frost. Interleukin-2 production by tumor cells bypasses T helper function in the generation of an antitumor response. *Cell* 60:397-403 (1990).
21. B. Gansbacher, K. Zier, B. Daniels, K. Cronin, R. Bannerji, and E. Gilboa. Interleukin 2 gene transfer into tumor cells abrogates tumorigenicity and induces protective immunity. *J. Exp. Med.* 172:1217-1224 (1990).
22. R. Bannerji, C. D. Arroyo, C. Cordon-Cardo, and E. Gilboa. The role of IL-2 secreted from genetically modified tumor cells in the establishment of antitumor immunity. *J. Immunol.* 152:2324-2332 (1994).
23. K. Morikawa, F. Okada, M. Hosokawa, and H. Koybayashi. Enhancement of therapeutic effects of recombinant interleukin-2 on a transplantable rat fibrosarcoma by the use of a sustained release vehicle, pluronic gel. *Cancer Res.* 54:182-189 (1987).
24. L.-S. Liu, S.-Q. Liu, S. Y. Ng, M. Froix, and J. Heller. Controlled release of interleukin-2 for tumour

- immunotherapy using alginate/ chitosan porous microspheres. *J. Control. Release* 30:241251 (1997).
25. N. K. Egilmez, Y. S. Jong, Y. Iwanuma, J. S. Jacob, C. A. Santos, F. A. Chen, E. Mathiowitz, and R. B. Bankert. Cytokine immunotherapy of cancer with controlled release biodegradable microspheres in a human tumor xenograft/SCID mouse model. *Cancer Immunol. Immunother.* 46:21-24 (1998).
26. P. Sampath, J. Hanes, F. DiMeco, B. M. Tyler, D. Brat, D. M. Pardoll, and H. Brem. Paracrine immunotherapy with interleukin2 and local chemotherapy is synergistic in the treatment of experimental brain tumors. *Cancer Res.* 59:2107-2114 (1999).
27. M. Ingram, C. H. Shelden, S. Jacques, R. G. Skillen, W. G. Bradley, G. B. Techy, D. B. Freshwater, R. M. Abts, and R. W. Rand. Preliminary clinical trial of immunotherapy for malignant glioma. *J. Biol. Response Mod.* 6:489-498 (1987).
28. S. C. Saris, P. Spiess, D. M. Lieberman, S. Lin, S. Walbridge, and E. H. Oldfield. Treatment of murine primary brain tumors with systemic interleukin-2 and tumor-infiltrating lymphocytes. *J. Neurosurg.* 76:513-519 (1992).
29. G. E. Plautz, G. H. Barnett, D. W. Miller, B. H. Cohen, R. A. Prayson, J. C. Krauss, M. Luciano, D. B. Kangisser, and S. Shu. Systemic T cell adoptive immunotherapy of malignant gliomas. *J. Neurosurg.* 89:42-51 (1998).
30. J. I. Mayordomo, T. Zorina, W. J. Storkus, L. Zitvogel, C. Celluzzi, L. D. Falo, C. J. Melief, S. T. Ildstad, W. M. Kast, A. B. Deleo, and M. T. Lotze. Bone marrow-derived dendritic cells pulsed with synthetic tumour peptides elicit protective and therapeutic antitumor immunity. *Nature Med.* 1:1297-1302 (1995).

[Author Affiliation]

Justin Hanes,^{1,2,7} Allen Sills,² Zhong Zhao,³ Kwang Wook Suh,^{4,9} Betty Tyler,² Francesco DiMeco,^{2,6} Daniel J. Brat,^{5,8} Michael A. Choti,⁴ Kam W. Leong,³ Drew M. Pardoll,¹ and Henry Brem^{1,2,10}

¹ Departments of Oncology, The Johns Hopkins University School of Medicine, Baltimore, Maryland 21205.

² Neurosurgery, The Johns Hopkins University School of Medicine, Baltimore, Maryland 21205.

³ Biomedical Engineering, The Johns Hopkins University School of Medicine, Baltimore, Maryland 21205.

⁴ Surgery, The Johns Hopkins University School of Medicine, Baltimore, Maryland 21205.

⁵ Neuropathology, The Johns Hopkins University School of Medicine, Baltimore, Maryland 21205.

⁶ Istituto Nazionale Neurologico "C.Besta," Milan, Italy.

⁷ Current address: Department of Chemical Engineering, Johns Hopkins University.

⁸ Current address: Department of Pathology, Emory University School of Medicine.

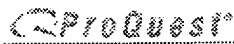
⁹ Department of Surgery, Ajou University School of Medicine, Suwon, Korea.

¹⁰ To whom correspondence should be addressed. (e-mail: hbrem@jhmi.edu)

Copyright © 2003 ProQuest Information and Learning Company. All rights reserved. [Terms and Conditions](#)

Text-only interface

From: ProQuest

[« Back to Article View](#)

Databases selected: Multiple databases...

Regional methionine and glucose uptake in high-grade gliomas: A comparative study on PET-guided stereotactic biopsy

Serge Goldman, Marc Levivier, Benoit Pirotte, Jean-Marie Brucher, et al. *The Journal of Nuclear Medicine*. New York: Sep 1997. Vol. 38, Iss. 9; pg. 1459, 4 pgs

Author(s): Serge Goldman, Marc Levivier, Benoit Pirotte, Jean-Marie Brucher, et al

Publication title: *The Journal of Nuclear Medicine*. New York: Sep 1997. Vol. 38, Iss. 9; pg. 1459, 4 pgs

Source Type: Periodical

ISSN/ISBN: 01615505

ProQuest document ID: 14403386

Text Word Count 3229

Article URL: http://gateway.proquest.com/openurl?ctx_ver=z39.88-2003&res_id=xri:pqd&rft_val_fmt=ori:fmt:kev:mtx:journal&genre=article&rft_id=xri:pqd:did=000000014403386&svc_dat=xri:pqi:fmt=htm&lreq_dat=xri:pqi:pq_clntid=19649

Full Text (3229 words)*Copyright Society of Nuclear Medicine Sep 1997*

[Headnote]

Serge Goldman, Marc Levivier, Benoit Pirotte, Jean-Marie Brucher, David Wikler, Philippe Damhaut, Sophie Dethy, Jacques Brotchi and Jerzy Hildebrand
PET/Biomedical Cyclotron Unit, Service de Neurologie and Service de Neurochirurgie, ULB-Hopital Erasme; and Department of Neuropathology, Cliniques Universitaires Saint-Luc, Brussels, Belgium

[Headnote]

Gliomas are regionally heterogeneous tumors. The local relationship between histologic features and radiotracer uptake evaluated by PET should therefore influence analysis and interpretation of PET results on gliomas. This study explored this local relationship as a result of PET guidance of stereotactic biopsies. Methods: Local histology was confronted to the regional uptake of ¹⁸F-2-fluoro-2-deoxy-D-glucose (¹⁸F-FDG) and ¹¹C-methionine (¹¹C-MET) in 14 patients with high-grade glioma diagnosed during a procedure of PET-guided stereotactic biopsies. We analyzed the uptake of both tracers in regions of interest centered on the stereotactic coordinates of 93 biopsy samples. Results: A semiquantitative analysis revealed a significant regional correlation between ¹¹C-MET and ¹⁸F-FDG uptakes. Uptake of both tracers was significantly higher on the site of tumor samples showing anaplastic changes than in the rest of the tumor. Presence of necrosis in anaplastic areas of the tumor significantly reduced the uptake of ¹¹C-MET. Conclusion: PET with ¹¹C-MET and ¹⁸F-FDG may help to evaluate, in vivo, the metabolic heterogeneity of human gliomas. Anaplasia is a factor of increased uptake of both tracers, but microscopic necrosis in anaplastic areas influences their uptake differently. This finding probably relates to the differences in tracer uptake by non-neoplastic components of necrotic tumors. These results underline the complementary role of ¹⁸F-FDG and ¹¹C-MET for the study of brain tumors and favors their use for stereotactic PET guidance of diagnostic or therapeutic procedures.

Key Words: glioma; PET; fluorine-18-fluorodeoxyglucose; methionine; stereotaxy
J Nucl Med 1997; 38:14591462

Different radiotracers have been used with PET to help in the management of patients with glioma (1,2). These tracers may be classified into three groups: the markers of energetic metabolic pathways, the markers of protein and nucleic acid synthetic pathways and the radioligands for receptor imaging. Most investigators use tracers from the two first classes, e.g., ¹⁸F-2-fluoro-2-deoxy-D-glucose (¹⁸F-FDG) which assays glucose metabolism, and ¹¹C-methionine (¹¹C-MET) or other amino acid tracers, which assay amino acid transport and metabolism (3-7). Tracer choice depends on

the goals pursued which may involve diagnosis, lesion delineation, grade and prognosis estimation and evaluation or prediction of response to treatment. For instance, it has been claimed that, for the definition of tumor limits, PET with ^{11}C -MET (MET-PET) is better than PET with ^{18}F -FDG (FDG-PET) or other modalities such as CT and MRI (8,9). To compare the characteristics of different PET tracers, it is essential to ascertain that the brain regions investigated during different PET procedures are similar, a condition which may be fulfilled using matching (10) or preferably stereotactic methods (8,11-13). Another important requisite for these comparative analyses is the definition, on the brain images, of regions of interest (ROIs) which adequately sample the tumor tissue. Since areas of high tracer uptake may be different with diverse tracers and since other imaging modalities, such as MRI, cannot ensure where the limits of the tumor are (9), histologic control of the regions concerned by the analysis seem to offer the best guarantee that this requirement is achieved. Furthermore, this histologic control allows confrontation of the multiple metabolic data with pathological features of the tumor. Therefore, we decided to apply a procedure of PET-guided stereotactic biopsies (II) to the comparison and histologic confrontation of PET information provided by two major tumor tracers used for the management of brain tumors: ^{18}F -FDG and ^{11}C -MET.

MATERIALS AND METHODS

Patients

A consecutive series of 19 patients suspected of having a brain tumor gave informed consent to undergo stereotactic biopsies guided by CT and by PET with successive injection of ^{11}C -MET and ^{18}F -FDG after a procedure which allows image data acquisition (stereotactic CT and PET), surgical planning and biopsies on the same day, as described in detail elsewhere (11). The analysis was conducted on 14 patients with a diagnosis of high-grade glioma (Table 1). Diagnosis in the patients not included in the analysis was low-grade astrocytoma ($n = 1$), metastasis from undifferentiated tumor ($n = 2$), gliosis from undetermined origin ($n = 1$) and vascular lesion ($n = 1$).

In all patients, we obtained the PET scans (15 6.75-mm-thick adjacent slices, eight direct and seven crossed slices, covered the entire brain) in stereotactic conditions after a protocol previously described (11,14). The patients were fasted, conscious, in a supine resting state with eyes closed and ears unplugged. The in-plane spatial resolution (FWHM) was about 5 mm. During PET acquisition, the stereotactic head-ring was secured to the clamp, which fits both into the CT and into the PET couch. The fiducial reference system used for stereotactic PET consisted of V-shape tubing filled with an ^{18}F -fluoride solution adapted on four localization plates originally designed for stereotactic MRI. Before the emission scans, a transmission scan was obtained using a ring source filled with an ^{18}F -fluoride solution and allowing a measured correction of the images for attenuation. The subjects were first injected intravenously with a bolus of 370-550 MBq (10-15 mCi) ^{11}C -MET prepared with an automated synthesis system after the procedure described by Comar et al. (15,16), and an image was acquired from 20-40 min postinjection. At least 80 min after the ^{11}C -MET injection, each patient was injected with a bolus of about 260 MBq (7 mCi) ^{18}F -FDG prepared after the method of Hamacher et al. (17). The delay between both injections ensured negligible contamination of the PET-FDG images by residual ^{11}C radioactivity. Static PET-FDG images were acquired from 40-60 min postinjection.

To estimate the radioactive content at the level of each biopsy sample site, circular 0.3 cm^2 ROIs were centered on the coordinates of the actual biopsy recorded postoperatively and transferred on the stereotactic MET-PET and FDG-PET using a local implementation of the PET processing software.

As previously described (IS), we evaluated radioactive content in noninvolved gray matter using ROIs

delineated in the frontal and temporal cortex of the hemisphere contralateral to the tumor. We calculated the mean counting rates in the ROIs distributed in the cortex. These mean counting rates were weighted for the number of pixels in each ROI and used to calculate tumor-to-cortex ratios. A total of 93 cylindrical tumor biopsy specimens (diameter = 1 mm, length = 1 cm) were obtained from the serial stereotactic biopsies performed with a side-cutting cannula after the technique described by Kelly et al. (19). After formalin-fixation and embedding, serial sections were obtained and stained with hematoxylin and eosin, Masson's trichrome and some immunostains (glial fibrillary acidic protein, S-100 protein, neuron-specific enolase, vimentin and others) when necessary (20). Presence or absence of nonexclusive histologic features were recorded in all samples: infiltrating tumor cells in brain tissue surrounding a tumor, anaplasia, focal microscopic necrosis and extensive microscopic necrosis.

Statistical analysis involved Spearman correlation coefficient, Kruskal-Wallis test and Mann-Whitney U-test without correction for multiple comparisons.

RESULTS

In the total set of 93 tumor samples, tumor-to-cortex ratios calculated on MET-PET and FDG-PET were highly positively correlated (Fig. 1, Spearman rho = 0.77, $p < 0.0001$).

The tumor samples were divided into three categories in function of histologic characteristics: samples with typical anaplastic changes ($n = 63$), samples from nonanaplastic areas of the tumor ($n = 19$) and samples with only infiltrating tumor cells in brain tissue ($n = 13$). The three categories of samples had significantly different values of tumor-to-cortex ratios calculated on MET-PET (Kruskal-Wallis, $p < 0.0001$). Similar differences between samples from the three categories were also found on FDG-PET (Table 2). In both MET-PET and FDG-PET, these differences were due to the higher values at the level of anaplastic samples compared to nonanaplastic samples and samples with infiltrating tumor cells. Levels of tracer uptake relative to the cortex were different for MET-PET and FDG-PET. The mean tumor-to-cortex ratio was higher than one in all three groups of tumor samples for MET-PET but only in the group of anaplastic samples for FDG-PET. Figure 2 illustrates the higher uptake of both tracers in the anaplastic area of the tumor in a patient with anaplastic astrocytoma. This case also illustrates the presence of elevated uptake of ^{11}C -MET in nonanaplastic areas of the tumor where ^{18}F -FDG appears reduced relatively to the cortex.

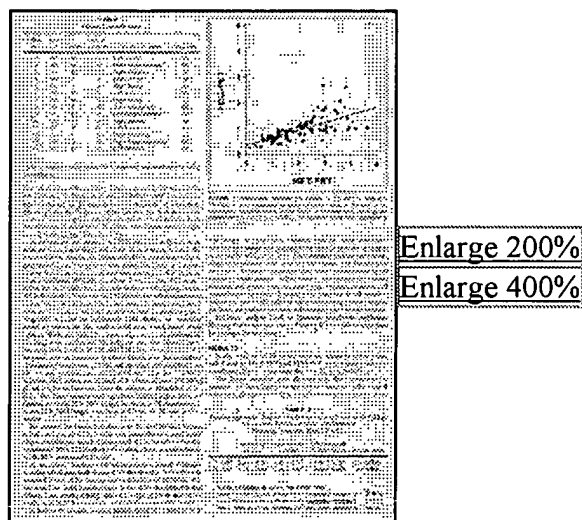


TABLE FIGURE TABLE 2

Presence of focal or extensive necrosis at the level of anaplastic samples significantly reduced

tumor-to-cortex ratios calculated on MET-PET (Kruskal-Wallis, $p < 0.005$). Such a significant effect of necrosis was not found on FDG-PET, even if lower values in the few samples with extensive necrosis were noticed (Table 3). When samples with focal and extensive necrosis were grouped in the statistical analysis, tumor-to-cortex ratios were significantly lower at the level of samples with necrosis on MET-PET (Mann-Whitney U test, $p < 0.005$) but not on FDG-PET (Fig. 3).

DISCUSSION

This study shows a correlated increase in ^{11}C -MET and ^{18}F -FDG uptake in anaplastic areas of malignant human gliomas. The ratio method used for semiquantification of the images generates directly comparable results for the two tracers. Despite the normalization inherent to the method, it does not provide, however, common thresholds of uptake for the two tracers. Indeed, normal gray matter presents a high uptake of FDG while its uptake of methionine is relatively low. Simple relative quantification instead of absolute quantification is justified by previous results obtained in a different series of patients and which has showed that, for ^{18}F -FDG, the simple ratio method is as effective as local glucose metabolic rate calculation for the differentiation between anaplastic and nonanaplastic areas of brain tumors (21). Furthermore, some investigations on human brain tumors have refuted assumptions on the lumped constant which corrects for the difference in transport and phosphorylation rates between glucose and 18FFDG for quantification by autoradiographic and graphical methods (1,22). In addition, the actual local glucose concentration in the tumor capillaries, necessary for metabolic rate quantification and estimated from the peripheral arterial plasma level, varies probably regionally in the tumor in function of the local glycolysis stimulation. Similarly, the biochemical mechanisms that govern the uptake of ^{11}C -MET in brain tumors have not been clarified yet, and the methods proposed for the quantification of this uptake doubtfully provide metabolic rates of a single biochemical process (23,24). Our study, under histologic control, demonstrates that the uptakes of ^{11}C -MET and ^{18}F -FDG are heterogeneous within the limits of a malignant glioma. The heterogeneity demonstrated in vivo by PET probably represents the metabolic counterpart of the well-known histologic heterogeneity of gliomas (25). Similar influence of anaplastic changes on the uptake of the two tracers probably explains the correlation found between the two uptake ratios in the whole series of tumor samples.

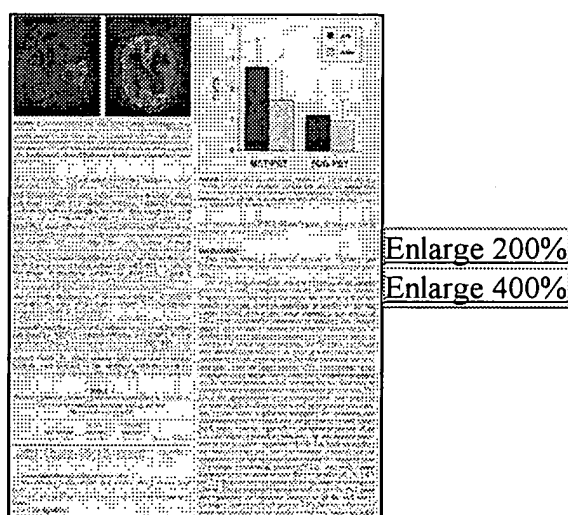


FIGURE 2. TABLE 3 FIGURE 3.

The relationship between local glucose consumption and anaplasia, a major predictor of survival in glial tumors (2, probably originates in the abnormal induction of glycolysis in malignant proliferating cells, partly as a consequence of overexpression of glucose transporters (27,28). On the other hand, total dependence of ^{11}C -MET uptake on the proliferative activity of human gliomas seems

contradicted by the increased uptake demonstrated by PET in various low-grade gliomas (4-6,29). Nevertheless, non-CNS tumor models have revealed influence of proliferative activity on methionine uptake which might explain the higher uptake in anaplastic zones in our series of tumor (30,31). Furthermore, previous PET studies have revealed higher global ^{11}C -MET uptake in high-grade than in low-grade gliomas (4-6,29).

Our analysis is based on a method of PET-guided stereotactic biopsy that we have initially developed and validated with ^{18}F -FDG (11,14). This study demonstrates that ^{11}C -MET offers a worthy alternative for the PET guidance of stereotactic diagnostic or therapeutic procedures towards the anaplastic components of the tumor. Compared to ^{18}F -FDG, ^{11}C -MET presents the advantage of a better detection of nonanaplastic tumor zones and of brain regions with infiltrating neoplastic cells. This advantage is valuable when a stereotactic procedure aims at a volumetric resection based on imaging information. Another advantage of ^{11}C -MET compared to ^{11}F -FDG is the more reliable differentiation of tumor from gray matter. Nevertheless, ^{18}F -FDG may remain the tracer of choice to image contrast-enhanced lesions on CT or MRI, since blood-brain barrier alteration has minimal influence on FDG-PET (1,32,33) but might interfere with ^{11}C -MET uptake (23,24,34).

We observe a reduction in ^{11}C -MET but not ^{18}F -FDG uptake at the level of tumor areas with necrotic components. This observation parallels recent microautoradiographic results on animal non-CNS cancer models showing that uptake of ^{14}C -labeled methionine is proportional to the amount of viable tumor cells and is low in macrophages and other non-neoplastic cellular components (30). On the other hand, several microautoradiographic experiments have revealed high uptake of ^{18}F -FDG in tumor-associated macrophages and preneoplastic cells (30,35). We have previously attributed to the same phenomenon the better survival of patients with glioblastoma in whom a first cycle of chemotherapy induces a hypermetabolic reaction (18). This uptake of tracer in cellular components related to the necrotic process might explain our present results of maintained ^{18}F -FDG uptake in anaplastic areas with necrosis.

CONCLUSION

This stereotactic PET study in human gliomas shows parallel anatomical heterogeneity of ^{11}C -MET and ^{18}F -FDG uptakes and influence of anaplastic changes on the uptake of these tracers. Non-neoplastic cellular components are probably implicated in the different influence of necrotic changes in MET-PET and FDG-PET. These results emphasize the complementary role of ^{18}F -FDG and ^{11}C -MET for the study of brain tumors. They support the use of either ^{18}F -FDG or ^{11}C -MET for the stereotactic PET guidance of diagnostic and therapeutic procedures.

ACKNOWLEDGMENTS

This study was supported by grants 9.4503.91 and 9.4513.93F from the Belgian National Lottery and 3.4509.92, 3.4508.92 and 3.4532.94 from the National Funds for Scientific Research, Belgium.

[Reference]

REFERENCES

[Reference]

1. Herholz K, Wienhard K, Heiss WD. Validity of PET studies in brain tumors. *Cerebrovasc Brain Metab Rev* 1990;2:240-265.
2. Coleman RE, Hoffman JM, Hanson MW, et al. Clinical application of PET for the evaluation of brain tumors. *J Nucl Med* 1991;32:616-622.
3. Di Chiro G, DeLaPaz RL, Brooks RA, et al. Glucose utilization of cerebral gliomas measured by ^{18}F -FDG and PET. *Neurology* 1982;32:1323-1329.
4. Bustany P, Chatel M, Derlon JM, et al. Brain tumor protein synthesis and histological grades: a study by PET with ^{14}C -L-methionine. *J Neurooncol* 1986;3:397-404.
5. Derlon JM, Bourdet C, Bustany P, et al. Carbon-11-L-methionine uptake in gliomas. *Neurosurgery* 1989;25:720-728.
6. Ogawa T, Shishido F, Kanno I, et al. Cerebral glioma: evaluation with methionine PET. *Radiology*, 1993;186:45-53.
7. Wienhard K, Herholz K, Coenen HH, et al. Increased amino acid transport into brain tumors measured by PET of L-(2- ^{18}F)fluorotyrosine. *J Nucl Med* 1991;32:1338-1346.
8. Bergstrom M, Collins VP, Ehrin E, et al. Discrepancies in brain tumor extent as shown by computed tomography and PET using ^{68}Ga -EDTA, ^{14}C -glucose and L-C-methionine. *J Comput Assist Tomogr* 1983;7:1062-1066.
9. Tovi M, Lilja A, Bergstrom M, et al. Delineation of gliomas with magnetic resonance imaging using Gd-DTPA in comparison with computed tomography and PET. *Acta Radiology* 1990;31:417-429.

[Reference]

10. Herholz K, Pietrzyk U, Voges J, et al. Correlation of glucose consumption and tumor cell density in astrocytomas: a stereotactic PET study. *J Neurosurg* 1993;79:853-858.
11. Levivier M, Goldman S, Bidaut LM, et al. PET-guided stereotactic brain biopsy. *Neurosurgery* 1992;31:792-797.
12. Thomas DGT, Gill SS, Wilson C. Current and future utilization of PET scanning in the evaluation and management of malignant cerebral glioma. In: M.L.J. Appuzzo, ed. *Malignant cerebral glioma*. Park Ridge, IL: American Association of Neurological Surgeons 1991;79-89.
13. Maciunas RJ, Kessler RM, Maurer C, et al. PET imaging directed stereotactic neurosurgery. *Stereotact Funct. Neurosurg* 1992;58:134-140.
14. Levivier M, Goldman S, Pirotte B, et al. Diagnostic yield of stereotactic brain biopsy guided by PET with ^{18}F -fluorodeoxyglucose. *J Neurosurg* 1995;82:445-452.
15. Comar D, Cartron J-C, Maziere M, Marazano C. Labeling and metabolism of ^{11}C -methionine methyl. *Eur J Nucl Med* 1976;1:11-14.
16. Dethy S, Goldman S, Blecic S, et al. Carbon-11-methionine and ^{18}F -FDG PET study in brain hematoma. *J Nucl Med* 1994;35:1162-1166.
17. Hamacher K, Coenen HH, Stocklin G. Efficient stereospecific synthesis of no-carrier-added 2- ^{18}F fluoro-2-deoxy-D-glucose using aminopolyether supported nucleophilic substitution. *J Nucl Med* 1986;27:235-238.
18. De Witte O, Hildebrand J, Luxen A, Goldman S. Acute effect of carmustine on glucose metabolism in brain and glioblastoma. *Cancer* 1994;74:2836-2842.
19. Kelly PJ, Daumas-Duport C, Kispert DB, et al. Imaging-based stereotactic serial biopsies in untreated intracranial glial neoplasms. *J Neurosurg* 1987;66:865-874.
20. Brucher J-M. Neuropathological diagnosis with stereotactic biopsies. Possibilities, difficulties and requirements. *Acta Neurochir (Wien)* 1993;124:37-39.

[Reference]

21. Goldman S, Levivier M, Pirotte B, et al. Regional glucose metabolism and histopathology of gliomas: a study based on positron emission tomography-guided stereotactic biopsy. *Cancer* 1996;78:1098-1106.
22. Junck L, McKeever PE, Ross DA, et al. The significance of fluorodeoxyglucose uptake in gliomas [Abstract]. *J Cereb Blood Flow Metab* 1995;15:S737.
23. Meyer G-J, Van den Hoff J, Borchert W, Hundeshagen H. Approaches to quantitative analysis of amino acid transport and metabolism. In: Mazoyer BM, Heiss WD and Comar D, eds. *PET studies on amino acid metabolism and protein synthesis*. Dordrecht: Kluwer Academic Publishers; 1993:183-196.
24. Ishiwata K, Kubota K, Murakami M, et al. Re-evaluation of amino acid PET studies: can the protein synthesis rates in brain and tumor tissues be measured in vivo? *J Nucl Med* 1993;34:1936-1943.
25. Paulus W, Peiffer J. Intratumoral histologic heterogeneity of gliomas: a quantitative study. *Cancer* 1989;64:442-447.
26. Daumas-Duport C, Scheithauer BW, O'Fallon JF, Kelly PJ. Grading of astrocytomas: a simple and reproducible method. *Cancer* 1988;62:2152-2165.
27. Warburg O. In: *The metabolism of tumors*. London: Arnold Constable 1930;75-327.
28. Yamamoto T, Seino Y, Fukumoto H, et al. Overexpression of facilitate glucose transporter genes in human cancer. *Biochem Biophys Res Commun* 1990;170:223-230.
29. Mosskin M, von-Holst H, Bergstrom M, et al. PET with ^{11}C -methionine and computed tomography of intracranial tumors compared with histopathologic examination of multiple biopsies. *Acta Radiol* 1987;28:673-681.
30. Kubota R, Kubota K, Yamada S, et al. Methionine uptake by tumor tissue: a microautoradiographic comparison with FDG. *J Nucl Med* 1995;36:484-492.

[Reference]


31. Miyazawa H, Arai T, Iio M, Hara T. PET imaging of non-small-cell lung carcinoma with carbon-11-methionine: relationship between radioactivity uptake and flowcytometric parameters. *J Nucl Med* 1993;34:1886-1891. 32. Hawkins RA, Phelps ME, Huang SC. Effects of temporal sampling, glucose metabolic rates and disruptions of the blood-brain barrier on the FDG model with and without a vascular compartment: studies in human brain tumors with PET. *J Cereb Blood Flow Metab* 1986;6:170-183.
33. Herholz K, Rudolf J, Heiss WD. FDG transport and phosphorylation in human gliomas measured with dynamic PET. *J Neurooncol* 1992;12:159-165. 34. Roelcke U, Rad. EW, Leenders KL. Carbon-11 -methionine and ⁸²Rb uptake in human brain tumors: comparison of carrier dependent blood-brain barrier transport. In: Mazoyer BM, Heiss WD and Comar D, eds. *PET studies on amino acid metabolism and protein synthesis*. Dordrecht: Kluwer Academic Publishers; 1993;197-199. 35. Kubota R, Yamada S, Kubota K, et al. Intratumoral distribution of fluorine-18fluorodeoxyglucose in vivo: high accumulation in macrophages and granulation tissues studied by microautoradiography. *J Nucl Med* 1992;33:1972-1980.

[Author Affiliation]

Received Jan. 22, 1996; revision accepted Jul. 22, 1996. For correspondence or reprints contact: Serge Goldman, MD, PET/Biomedical Cyclotron Unit, ULB-Hopital Erasme, SOS, route de Lennik, B-1070 Brussels, Belgium.







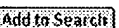




Copyright © 2003 ProQuest Information and Learning Company. All rights reserved. [Terms and Conditions](#)

Text-only interface

From:  ProQuest

Recent Searches

[Close window](#) | [Help](#)Add terms to your search using: 

- | | |
|---|--|
| 15. (microsphere) AND (stereotactic) AND (injection)
<i>Database:</i> Multiple databases...
<i>Limit results to:</i> full text
<i>Look for terms in:</i> Citation and article text
<i>Publication type:</i> All publication types | 1 result  |
| 14. (stereotatic injection) AND (microsphere)
<i>Database:</i> Multiple databases...
<i>Limit results to:</i> full text
<i>Look for terms in:</i> Citation and article text
<i>Publication type:</i> All publication types | 0 result  |
| 13. (stereostatic injection) AND (microsphere)
<i>Database:</i> Multiple databases...
<i>Limit results to:</i> full text
<i>Look for terms in:</i> Citation and article text
<i>Publication type:</i> All publication types | 0 result  |
| 12. (glioblastoma) AND (injection) AND (stereotactic)
<i>Database:</i> Multiple databases...
<i>Limit results to:</i> full text
<i>Look for terms in:</i> Citation and article text
<i>Publication type:</i> All publication types | 10 results  |
| 11. (cancer) AND (5-fluorouracil)
<i>Database:</i> Multiple databases...
<i>Limit results to:</i> full text
<i>Look for terms in:</i> Citation and article text
<i>Publication type:</i> All publication types | 1585 results  |
| 10. (cancer) AND (glioblastomas) AND (5-fluorouracil)
<i>Database:</i> Multiple databases...
<i>Limit results to:</i> full text
<i>Look for terms in:</i> Citation and article text
<i>Publication type:</i> All publication types | 0 result  |
| 9. (treating) AND (glioblastomas) AND (5-fluorouracil)
<i>Database:</i> Multiple databases...
<i>Limit results to:</i> full text
<i>Look for terms in:</i> Citation and article text
<i>Publication type:</i> All publication types | 0 result  |
| 8. (treatment) AND (ganglioma) AND (5-fluorouracil)
<i>Database:</i> Multiple databases...
<i>Limit results to:</i> full text
<i>Look for terms in:</i> Citation and article text
<i>Publication type:</i> All publication types | 0 result  |
| 7. AU(benoit) AND (injection) AND (stereotactic)
<i>Database:</i> Multiple databases...
<i>Limit results to:</i> full text
<i>Look for terms in:</i> Citation and article text
<i>Publication type:</i> All publication types | 1 result  |
| 6. AU(benoit) AND (tumor) AND (stereotactic)
<i>Database:</i> Multiple databases...
<i>Limit results to:</i> full text
<i>Look for terms in:</i> Citation and article text
<i>Publication type:</i> All publication types | 1 result  |
| 5. (anticancer agent) AND (tumor) AND (stereotactic) | 0 result  |

*Database:*Multiple databases...

Limit results to: full text

Look for terms in: Citation and article text

*Publication type:*All publication types

4. (microsphere) AND (tumor) AND (stereotactic)

0 result [Add to Search](#)

*Database:*Multiple databases...

Limit results to: full text

Look for terms in: Citation and article text

*Publication type:*All publication types

3. (microsphere) AND (tumor) AND (stereoactic)

0 result [Add to Search](#)

*Database:*Multiple databases...

Limit results to: full text

Look for terms in: Citation and article text

*Publication type:*All publication types

2. (microsphere) AND (tumor) AND (steretactic)

0 result [Add to Search](#)

*Database:*Multiple databases...

Limit results to: full text

Look for terms in: Citation and article text

*Publication type:*All publication types

1. AU(fubara)

1 result [Add to Search](#)

*Database:*Multiple databases...

Limit results to: full text

Look for terms in: Citation and abstract

*Publication type:*All publication types

[Close window](#) | [Help](#)

Set Name Query
side by side

Hit Count Set Name
result set

DB=USPT,PGPB,JPAB,EPAB,DWPI; PLUR=YES; OP=ADJ

<u>L19</u>	L18 and l15	51	<u>L19</u>
<u>L18</u>	l14 and l17	1309	<u>L18</u>
<u>L17</u>	5-fluorouracil or platinum agent or tax\$3	32506	<u>L17</u>
<u>L16</u>	anti cancer or anti-cancer	13051	<u>L16</u>
<u>L15</u>	stereotactic injection	1036	<u>L15</u>
<u>L14</u>	microsphere	26318	<u>L14</u>
<u>L13</u>	microsphere	26318	<u>L13</u>

DB=DWPI; PLUR=YES; OP=ADJ

<u>L12</u>	WO-200251388\$.did.	1	<u>L12</u>
------------	---------------------	---	------------

DB=USPT,PGPB,JPAB,EPAB,DWPI; PLUR=YES; OP=ADJ

<u>L11</u>	WO-200251388\$.did.	1	<u>L11</u>
<u>L10</u>	L9 and stereotactic	5	<u>L10</u>
<u>L9</u>	Benoit.inv.	3752	<u>L9</u>
<u>L8</u>	Benoit,inv.	0	<u>L8</u>
<u>L7</u>	L6 and (taxane or platinum agent or 5-fluorouracil)	3	<u>L7</u>
<u>L6</u>	l1 and tumor	67	<u>L6</u>
<u>L5</u>	L4 and l3 and l2	1	<u>L5</u>
<u>L4</u>	microsphere same polylactic acid	462	<u>L4</u>
<u>L3</u>	inoperable same cancer	301	<u>L3</u>
<u>L2</u>	inoperable same tumor	442	<u>L2</u>
<u>L1</u>	sterotactic	114	<u>L1</u>

END OF SEARCH HISTORY